

## EXPERIMENTAL AND NUMERICAL ANALYSIS OF DISCHARGE COEFFICIENT IN INTERNAL COMBUSTION ENGINE

Soriano B.S\* and Rech C.  
 \*Author for correspondence  
 Automotive Mechanical Engineering Department,  
 Lutheran University of Brazil  
 Av. Farroupilha, 8001, CEP , 92425-900, Canoas, RS, Brazil.  
 E-mail: soriano915@hotmail.com

Zancanaro, F. V. Jr. and Vielmo, H. A.  
 Mechanical Engineering Department  
 Federal University of Rio Grande do Sul  
 Rua Sarmiento Leite, 425, CEP 90050-170, Porto Alegre, RS, Brazil

### ABSTRACT

In order to improve the breathing capacity of the intake system, experimental and numerical investigations of discharge coefficient ( $C_D$ ) are performed in an internal combustion engine. For this paper an experimental test rig was developed to measure steady and transient flow. Steady experimental data was obtained for various valve lift and transient measurement with only the intake valve operating. The suction pressure was generated by a fan, and utilized as boundary condition for the numerical simulation. The air mass flow was measured with a commercial hot film anemometer sensor with appropriate time response. The angular position of the camshaft was measured with a rotary encoder with a resolution of 0.175 degree. A length gauge with an accuracy of  $\pm 0.2 \mu\text{m}$  was used to measure valve opening. The air mass sensor and the rotary encoder were connected to a data acquisition board (National Instruments 6221) and its original LabVIEW software. The numerical simulation uses the STAR-CCM+ commercial Finite Volumes CFD code. Regarding turbulence, computations were performed with Reynolds-Averaged Navier-Stokes Realizable Two-Layer  $k-\varepsilon$  model with hybrid treatment near the walls. A detailed mesh independence study was performed. The steady simulations were done for the same experimental valve lift, with a good agreement among results.

### INTRODUCTION

In internal combustion engines (ICE), the flow conditions inside the cylinder are critical for the combustion process [1].

These are determined by the intake port and valve geometry. The  $C_D$  measures the flow permeability in the engine intake system. The airflow through an intake port and valve may be characterized by the discharge conditions at the intake valve. For good mixture preparation and high combustion rate, a fresh charge should have suitable large scale charge motion in the cylinder, e.g. swirl and tumble and the term microstructure of the turbulence intensity, which determine the flame penetration speed. These conditions depend on the geometry of the intake system, intake valve and engine operational parameters. Gosman et al. [2] showed that the tangential motion around the valve stem and head induced by the shroud forces the flow to exit at a larger angle than the valve seat angle resulting in flow separation at the valve sealing face.

A valve and its associated port are said efficient if there is minimal discrepancy between the effective or actual flow area and the geometrical flow area. This efficiency is quantitated by means of discharge or flow coefficient defined as the ratio of the actual flow area to the geometrical flow area [3].  $C_D$  of the inlet valve is influenced by the following factors: valve seat width, valve seat angle, rounding of seat corners, port design and cylinder head shape [1]. The air flow rate through the intake valve varies with intake pressure ratio, increasing as the pressure ratio increases [4-6]. Deep and detailed research on the in-cylinder gas flow produced during the intake process is helpful for achieving its efficient control and utilization in order to improve combustion, enhance performance and reduce emissions when developing engines.

There are many techniques to analyse the flow into the cylinder from experimental measures. For example, the Laser Induced Photochemical Anemometry (LIPA) [7], Laser Doppler Velocimetry (LDV) and hot wire/film anemometer.

The LDV technique can characterize the movement of mass air during the four strokes of the ICE. Although this is expensive equipment, it can measure the velocity field inside the cylinder while the engine is working. [8-13]. A hot wire anemometer can be used to measure the velocity profile and turbulence intensity in the discharge of a typical engine in steady operation [14]. The authors concluded that the velocity profile and turbulence intensity are strongly dependent on the valve opening and the geometry of the intake port. The methodology was utilized to measure the magnitude of angular momentum and swirl ratios in the admission process for each speed related with opening of valves [15]. A comparison between LDV and hot wire anemometer measurement was made [16]. The author's conclusion was that the use of laser Doppler allows a better resolution of the measurement, due to a larger scan of the geometry studied.

The  $C_D$  in a Diesel ICE is studied computationally to assess the capability of Computational Fluid Dynamics (CFD) in assisting experimental calibration. This paper focuses on a steady state regime that occurs in the flow permeability tests of a Diesel engine intake system [17,18].

The steady flow data are representative of the dynamic flow behavior of the valve in an operating engine. The pressure upstream of the valve varies significantly during the intake process. However, it has been shown that over the normal engine speed range, steady flow discharge coefficient results can be used to predict dynamics performance with reasonable precision [1].

During the last years more numerical simulations have been done regarding the  $C_D$  [19], focusing in directed intake port types, including comparisons with experimental measurements. With the growing availability of turbulent models and computational resources, many works make comparisons, regarding their capacity of reproduce experimental data and CPU time demanding.

Keeping the popular  $k-\varepsilon$  family, some works have been analyzing the alternatives for the stress-strain relationship, considering the compressible, non-isothermal, anisotropic effects presents in the ICE three-dimensional flows. For ICE case, the relation that provided the best agreement with data was cubic stress-strain [20]. In another work [21] the same authors investigated the High Reynolds and Low Reynolds near wall approaches, both with a cubic relationship between Reynolds stresses and strains. It was concluded that the Low Reynolds approach (boundary layer also discretized by the mesh), although increasing the computational effort, presented more ability in capturing the tested ICE intake flow.

An alternative is to use RNG models instead of nonlinear ones, considering its underlying concepts similar to nonlinear models, but with more objective simplicity. To obtain a better experimental agreement on engine flow, modify the RNG constants is another valid possibility [22].

In this work, experimental measurement of transient and steady air-mass flow in the intake system are made. The steady results of air-mass flow were converted to  $C_D$  and compared with simulation results of STAR-CD software.

## NOMENCLATURE

$\dot{m}_{actual}$	[kg/s]	Air-mass flow
$C_D$	[ ]	Discharge coefficient
$d_v$	[m]	Inner valve diameter
$R$	[J/kg-K]	Gas (air) constant
$T_o$	[K]	Stagnation (inlet) absolute temperature
$\gamma$	[ ]	Specific heat ratio
$p_{out}$	[Pa]	Pressure downstream of the valve
$p_{st}$	[Pa]	Stagnation pressure
$IVO$	[°]	Intake valve opening
$IVC$	[°]	Intake valve closing
$\theta$	[°]	Crankshaft angular position

## The Discharge Coefficient

The impact of a blockage on the engine breathing is assessed through a  $C_D$  that relates the actual mass flow rate through the intake valve to the isentropic mass flow rate. Therefore, the equation assumes the following form [1,23].

$$C_{D\_actual} = \frac{\dot{m}_{actual}}{\frac{\pi d_v^2}{4} \frac{p_{st}}{(RT_o)^{1/2}} \left(\frac{p_{out}}{p_{st}}\right)^{1/\gamma} \left\{ \frac{2\gamma}{\gamma-1} \left[ 1 - \left(\frac{p_{out}}{p_{st}}\right)^{(\gamma-1)/\gamma} \right] \right\}^{1/2}}$$

where  $\dot{m}_{actual}$  is obtained from the numerical solution, or experimentally. For this paper was assumed a constant passage area to calculate the theoretical mass flow rate. A global coefficient is obtained by integration along the crankshaft angle, as follows:

$$C_D = \frac{\int_{IVO}^{IVC} C_{D_i} d\theta}{IVC - IVO}$$

where  $\theta$  is a crankshaft angular position,  $IVO$  is the intake valve angle opening and  $IVC$  is the intake valve angle closing.

## NUMERICAL METHODOLOGY

The numerical solution was performed with Realizable Two-Layer  $k-\varepsilon$  model with hybrid treatment near the walls. This model combines the Realizable  $k-\varepsilon$  model with the two-layer All  $y+$  approach. The Two-Layer Wall All  $y+$  Treatment is a hybrid approach that seeks to recover the behaviors of the other two wall treatments in the limit of very fine or very coarse meshes. High- $y^+$  wall treatment is used for coarse meshes and the low- $y^+$  wall treatment for fine meshes. It is also formulated with the desirable characteristic of producing reasonable answers for meshes of intermediate resolution. [24].

Regarding the mesh, was used an unstructured hexahedral-trimmed cells with three prism layers of 0.3 mm of thickness and a stretching of 1.5. Fig. 1 and Fig. 2. A mesh independence study was performed, arriving about 350000 cells in the domain. The convergence criteria used for residuals was  $10^{-5}$ .

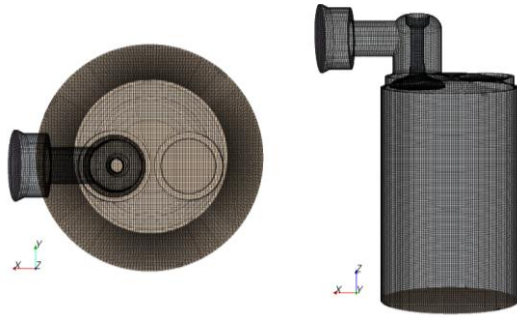


**Figure 1** - Unstructured hexahedral-trimmed mesh.

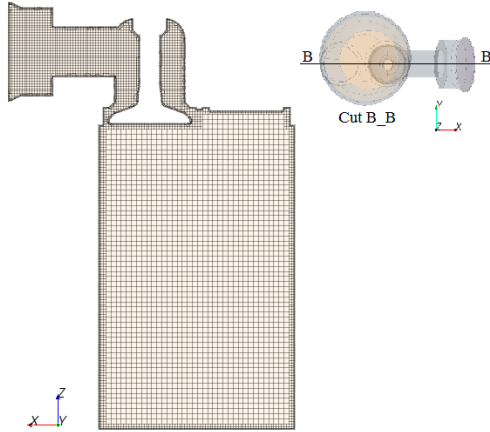


**Figure 2** - Unstructured hexahedral-trimmed mesh detail.

The boundary conditions are stagnation inlet and pressure outlet. The differencing scheme was the first order upwind. The suction pressure, at the outlet, was 10000 Pa, 8000 Pa and 6000 Pa. For all cases the temperature was 303 K, turbulence intensity  $I = 0.05$ , and length scale  $l = 0.01$  m, as a consequence of the flow and geometrical characteristics. Table 1 show the air properties for the temperature used in all simulations.

Table 1. Air properties for 303 K and 1 atm. [25]

Dynamic viscosity	1.872E-5 kg/m.s
Molecular weight	28.9664 kg/kg.mol
Specific heat	1007.0 J/kg.K
Thermal conductivity	0.02888 W/m.K

## EXPERIMENTAL METHODOLOGY

Transient and steady measurements system was made in the intake of a single cylinder four stroke engine Honda GX35. The specifications of the engine are given in the Table 2. The test bench for steady measurement includes the data acquisition board, the hot film anemometer, the electrical fan controlled by a voltage variator, the rotary encoder and a length gauge with an accuracy of  $\pm 0.2 \mu\text{m}$  (Heidenhain MT 25) [26]. The steady measurement was done for three different valve lift and a constant suction pressure downstream of the valve. Table 3

presents the three different valve lift utilized and its angular interval.

**Table 2.** Engine specifications. [27]

Honda GX35 engine	
Bore x Stroke [mm]	39 x 30
I/O/IVC [BTDC/ATDC]	25.41/66.21
Displacement [ $\text{cm}^3$ ]	35.8
Maximum valve lift [mm]	2.82
Intake air system	Naturally aspirated
Compression ratio	8:1

**Table 3.** Angular interval corresponding to each intake valve lift.

Intake valve lift [mm]	Angular interval $\Delta\theta$ [ $^\circ$ ]
1.000	41.967
2.000	30.059
2.500	21.929

For transient flow the camshaft was driven by an electrical motor, which provided the desired angular velocity of 115 rpm. The data was acquired with a commercial data acquisition board, National Instruments 6221 [28], and its original LabVIEW software [29]. The values of voltage and frequency were collected and processed with the correspondent characteristic curves of each sensor and converted into units of mass flow and angular position. It was acquired 2048 samples per revolution. The angular position of the camshaft was measured with an encoder sensor (Autonics E40S-6-2048-6-L-5) [30] supplying 2048 pulse per revolution.

The air-mass flow was measured downstream of the intake valve with an automotive hot film anemometer about 2 m of the valve port [31]. (MAF - Bosch 0 280 218 002). This sensor has an input voltage of 5 and 12 V. The output analogic signal is related to the air flow in the intake process. The incoming air dissipates heat from the hot film, so the higher the air flows, more heat is dissipated. The differential temperature is evaluated by an electronic hybrid circuit. So the air flow and its direction can be measured. Only part of the air-mass flow is registered by the sensor element. The total air mass flowing through the measuring tube is determined by means of calibration, known as the characteristic-curve definition [31]. The time constant of hot film anemometer, considering dynamic measurement, was determined in another work by authors [32], being verified that sensor is 8 times faster than necessary to measurements. The characteristic-curve, relating output voltage of the hot film anemometer and the air mass flow, was taken by an orifice plate. The schematic picture of the test bench is show in Figure 3.

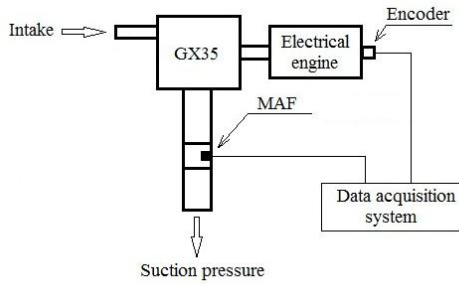


Figure 3 – Schematic picture of measurement system.

## ANALYSIS OF RESULTS

The experimental and numerical results are described in the Figure 4-6, according the valve lift. The Figure 7 presents the global  $C_D$ . The results present a good agreement, with maximum relative percentage error for the global  $C_D$  of 3.8% to 8000 Pa. As can be seen in the results, there is a very little dependence of the discharge coefficient on suction pressure.

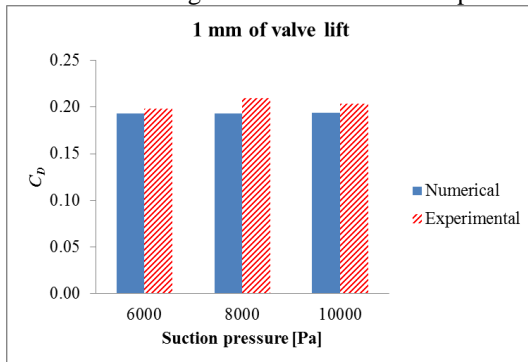


Figure 4 - Results for 1 mm valve lift.

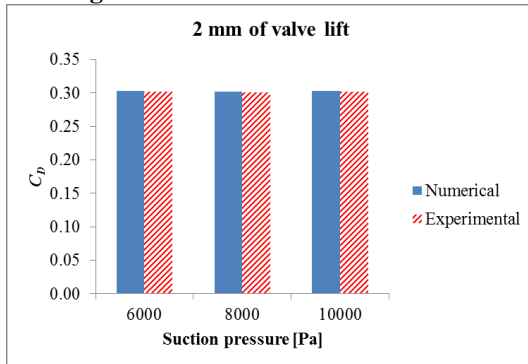


Figure 5 - Results for 2 mm valve lift.

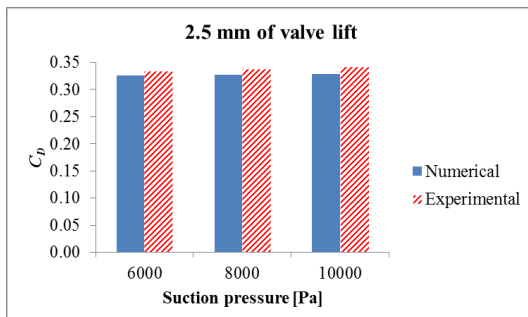


Figure 6 - Results for 2.5 mm valve lift.

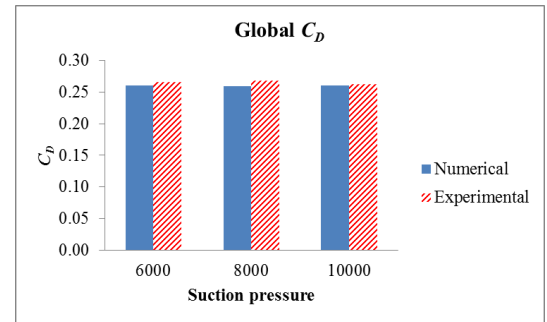


Figure 7 - Results for global  $C_D$ .

The Figure 8 shows the transient experimental results for 30 cycles of  $C_D$  in a motored internal combustion engine and its intake valve lift, as a function of crankcase angular position. The maximum mean standard deviation for this case was about 0.008, representing a good repeatability. The start of the acquisition was referred to the beginning of the intake valve opening. The global  $C_D$  for this case, with 10000 Pa of suction pressure, was 0.221.

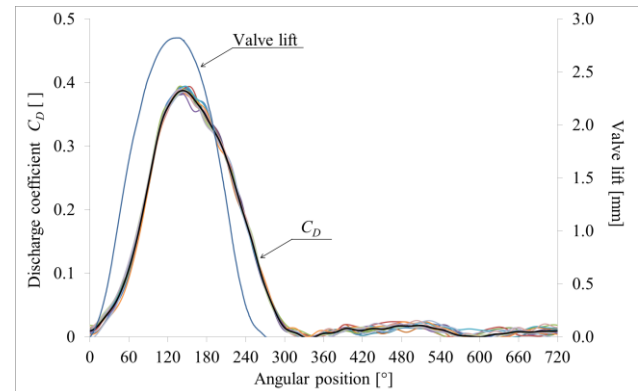


Figure 8 – Experimental results for air mass flow and valve lift.

The Figures 5 and 6 show the velocity vectors on sections A\_A and B\_B of the intake port at 2.5 mm valve lift and 6000 Pa suction pressure. It is detected a large recirculation flow, caused by the valve downstream low pressure. This large scale phenomenon is detected by all lift and suction pressure tested. It seems to be an intrinsic problem of four stroke internal combustion engines, and a potential cause for a reduction of discharge coefficient. The valve area restriction is the point of higher velocities and friction. Indeed, this restriction causes almost all of the pressures losses of the expansion.

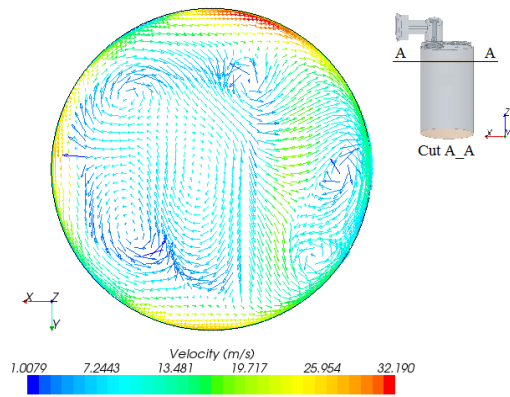


Figure 9. Velocity vectors on the cut A-A.

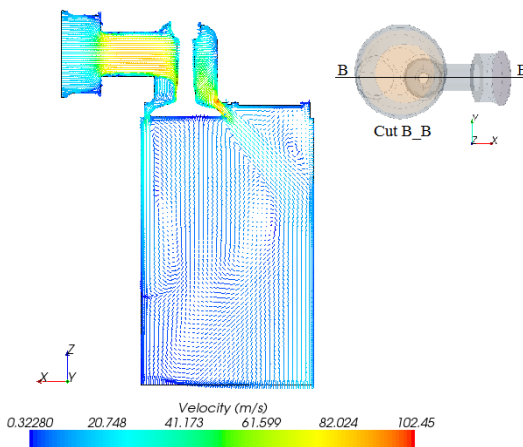


Figure 10. Velocity vectors on the cut B-B, seat valve region.

## CONCLUSION

The 3D turbulent, compressible flow in an internal combustion engine intake is solved. Comparisons between numerical and experimental data showed good agreement with maximum relative percentage error, for the global  $C_D$  of 3.8% to 8000 Pa.

One verifies that the discharge coefficient for each valve lift increases with increasing lift. The air flow rate through the intake valve varies with pressure ratio, increasing as the pressure ratio increases, as expected.

For the all the model investigated, the presence of recirculation in the port and in-cylinder are detected.

In the case of a practical application, considering that the objective is not to quantify the  $C_D$  but validate the numerical and experimental methodology, the objective was reached.

## REFERENCES

- [1] Heywood, J.B. Internal Combustion Engines. McGraw-Hill Inc. 1988.
- [2] Gosman, A.D., Tsui, Y.Y. and Vafidis, C., Flow in a model engine with a shrouded valve-a combined experimental and computational study. *SAE Technical Paper*, No.850498. 1985.

- [3] Ferguson, Colin R., Internal combustion engine. New York: J. Wiley, 1985.
- [4] Baratta, M.; Catania, A.E.; Pesce, F.C.; Spessa, E.; Rech C.; Vielmo, H.A., Multidimensional Modeling of a High Swirl-Generating Helical Intake Port for Diesel Engines, *12th Brazilian Congress of Thermal Engineering and Sciences, Belo Horizonte - MG, Proceedings of ENCIT*, Rio de Janeiro, RJ: ABCM, 2008
- [5] Zancanaro, F. V. Jr., Simulação Numérica do Escoamento Turbulento em Motores de Combustão Interna, Porto Alegre, UFRGS, *Dissertação de mestrado*, 2010.
- [6] Zancanaro, F. V. Jr., Vielmo, H.A., Intake Flow and Time Step Analysis in the Modeling of a Direct Injection Diesel Engine, *13th Brazilian Congress of Thermal Engineering and Sciences, Uberlândia - MG. Proceedings of ENCIT*, Rio de Janeiro, RJ: ABCM, 2010.
- [7] Stier B., Falco R.E., Application of LIPA (Laser Induced Photochemical Anemometry) to the Water Analog Model of a Four-Stroke IC Engine, *SAE Paper 940282*, 1994.
- [8] Uzman T, Borgnakke C, Morel T., Characterization of flow produced by a high-swirl inlet port. *SAE Paper 830266*, 1986.
- [9] Payri F, Desantes JM, Pastor JV. LDV measurements of the flow inside the combustion chamber of a 4-valve D.I. Diesel engine with axisymmetric piston bowls. *Experiments in Fluids*; Vol. 22:118–28, 1996.
- [10] F. Payri, J. Benajes, X. Margot, A. Gil. CFD modeling of the in-cylinder flow in direct-injection Diesel engines. Elsevier, *Computers & Fluids 33 (2004) 995–1021*.
- [11] Jaffri K, Hascher HG, Novak M, Lee K, Schock H, Bonne M, Tumble and swirl quantification within a motored four-valve SI engine cylinder based on 3-D LDV measurements. *SAE 970792*, 1997.
- [12] Corcione FE, Valentino G. Analysis of in-cylinder flow processes by LDA. *Combust Flame*; 99:387–94, 1994.
- [13] Hadded, O.; Denbratt, I., Turbulence characteristics of tumbling air motion in 4-valve SI engines and their correlation with combustion parameters, *SAE Paper 910478*, 1991.
- [14] Liu R., Xiao F., Guan L., X. L. Jilin, An Investigation into Air Flow Characteristics through Inlet Valve of Directed Ports, *SAE Paper 941753*, 1994.
- [15] Witze, P. O.; Hall, M. J.; Wallace, J. S., Fiber-optic instrumented spark plug for measuring early flame development in spark ignition engines, *SAE Paper 881638*, 1988.
- [16] Liu X., Liu R., Xiao F., Guan L., A Microscopic Analysis of In-Cylinder Swirl Generated by Directed Ports, *SAE Paper 941754*, 1994.
- [17] Fiat Research Center; Consiglio Nazionale delle Ricerche, Motore Monocilindro Diesel con Distribuzione a 2 Valvole e Protezioni Termiche Camera di Combustione. Contract N° 82.00047.93 (in italian), 1982.
- [18] Fiat Research Center; Consiglio Nazionale delle Ricerche, Metodologia per la Caratterizzazione dei Condotti di Aspirazione Motori in Flusso Stazionario. Contract N° 82.00047.93 (in italian), 1983.
- [19] Bianchi, G.M., Cantore, G. and Fontanesi, S., Turbulence Modeling in CFD Simulation of ICE Intake Flows: The Discharge Coefficient Prediction. *SAE Paper No 2002-01-1118*, 2002
- [20] Bianchi, G.M., Cantore, G., Parmeggiani, P. and Michelassi, V., On Application of Nonlinear  $k-\epsilon$  Models for Internal Combustion Engine Flows. *Transactions of the ASME vol. 124*, pp. 668-677, 2002.
- [21] Bianchi, G.M., Fontanesi, S., On the Applications of Low-Reynolds Cubic  $k-\epsilon$  Turbulence Models in 3D Simulations of ICE Intake Flows. *SAE Paper N° 2003-01-0003*, 2003.

- [22] Baratta, M., Catania, A.E., Spessa, E., and Liu, R.L., Multidimensional Predictions of In-Cylinder Turbulent Flows: Contribution to the Assessment of k- $\epsilon$  Turbulence Model Variants for Bowl-In-Piston Engines. *ASME J. of Eng. Gas Turbines Power*, 127, pp. 883-896, 2003.
- [23] Ferrari, G., *Motori a Combustione Interna*, Torino, Ed il Capitello, (in italian), 2005.
- [24] STAR-CCM+, User guide. 2012.
- [25] Yunus, A. Çengel, M. John, M. Fluid mechanics – Fundamentals and applications. 1<sup>o</sup>ed. – São Paulo: McGraw-Hill, 2007.
- [26] High-accuracy length gauges, 2012, “HEIDENHAIN-METRO MT25”,  
[https://www.valuetronics.com/Manuals/HEIDENHAIN\\_MT12-MT25B.pdf](https://www.valuetronics.com/Manuals/HEIDENHAIN_MT12-MT25B.pdf).
- [27] Honda Engines GX35, 2011, “model-detail/gx35”  
<http://engines.honda.com/models/model-detail/gx35>
- [28] National instruments, 2012, “NI PCI-6221”.  
<http://sine.ni.com/nips/cds/print/p/lang/en/nid/14132>.
- [29] Labview, 2008 “User guide” National Instruments.
- [30] Rotary encoder (incremental type), “E40S-6-2048-6-L-5 manual”.  
<http://autonics.thomasnet.com/Asset/E40S,HB,E80H%20manual.pdf>
- [31] Bosch, 2010 “Hot-film air-mass meter, type HFM 2”  
[http://apps.bosch.com.au/motorsport/downloads/sensors\\_airmass.pdf](http://apps.bosch.com.au/motorsport/downloads/sensors_airmass.pdf)
- [32] Soriano, B.; Rech, C. Low Cost Transient Discharge Coefficient Measure System. *21th International Congress of Mechanical Engineering, Natal – RN, Proceedings of COBEM*, Rio de Janeiro, RJ: ABCM, 2011.

## ACKNOWLEDGEMENTS

The authors thank the financial support from CNPq, Brazil, through a scientific productivity grant to Vielmo, H.A. and the CNPq Universal Project 470325/2011-9. Also a doctor scholarship grant to Zancanaro, F. V. Jr.

The authors thank the financial support from ULBRA Research, Brazil, through a scientific productivity grant to Rech, C.. and the Energetic Efficiency Project. Also a scientific initiation program scholarship grant to Soriano, B. S.